

Experimental Investigations of Mechanical Properties of Carbon Fiber Reinforced Polymers(CFRP) for structural applications

K.Karthik,N.Naveen Kumar,C.Nirmal Kumar,S.Harihara kumarean

Department Of Mechanical Engineering,K.Ramakrishnan College Of Engineering,Trichy

Abstract

This project presents the results of experimental studies about MS rod confined with high-strength carbon fiber reinforced polymer (CFRP) composites. Four small scale specimens (ID=25mm,OD=28.5mm) were subjected to uniaxial compression up to failure and stress-strain behaviours were recorded. The various parameters such as wrap thickness and fiber orientation were considered. The fiber orientation of 0° , 90° , 45° and combinations of them were investigated. The results demonstrated significant enhancement in the compressive strength, stiffness, and ductility of the CFRP-wrapped MS rod as compared to unconfined MS rod. The carbon fiber reinforced polymers (CFRP) used as an external wrapping is to achieve strengthening and repair of cylindrical structures. The CFRP composites have been used successfully for rehabilitation and strengthening of deficient reinforced cylindrical elements.Reinforced cylinder, need to be laterally confined in order to ensure large deformation under applied loads before failure and to provide an adequate strength.

Keywords: High strengthCFRP ; CFRP; Unconfined MS rod; Confined;External Wrapping ; Rehabilitation; Fibre Orientation; Axial Compression;

Nomenclature

f_{co}	Compressive strength of unconfined concrete	ϵ_{co}	Axial strain in strength of unconfined concrete	W/C	The water/cement ratio
f_{cc}	Compressive strength of CFRP confined concrete	ϵ_{cc}	Axial strain in strength of FRP- confined concrete	ϵ_{fu}	Ultimate FRP tensile strain
f_{cm}	Compressive average strength of concrete	ϵ_{cu}	Ultimate axial strain of CFRP-confined concrete	s	Standard deviation
f_l	Lateral confinement pressure	k_d	The effectiveness coefficient	n	Number of layers of the CFRP jacket
	Ultimate Confining pressure		Factor to the number of tests	n_i	CFRP volumetric ratio
t_j	Thickness of the CFRP jacket	E_f	Elastic modulus of the CFRP		total thickness of CFRP layer

1. Introduction

The application of composite materials in the reinforcement of concrete cylinder is an important topic in civil engineering , the advent of the fiber reinforced polymer (FRP) composites in the field of construction and structural applications was in the early 1950's, proprieties of FRP in comparison with steel : linear elastic behavior to failure, no yielding, higher ultimate strength, lower strain at failure, comparable modulus, high strength/Weight ratio, design flexibility, lightweight, corrosion resistance, low maintenance/long-term durability, tailored aesthetic appearance, dimensional stability, low thermal conductivity, corrosive resistant, impervious to chloride and chemical attack...etc .Used fiber FRP (composite) Such as (Steel-Aramid -Carbon /Graphite, Boron, S-Glass, E-Glass, Polypropylene, Polyethylene ... etc), in external applications on the surfaces of structural elements. Various parameters such as wrap thickness and fiber orientation were considered, different wrap thicknesses (1, 2, and 3 layers), fiber orientation of 0° , 90° , $\pm 45^\circ$, and their combinations were investigated whether to increase the capacity of those elements in the

investment stage or rehabilitation for an investment security and use some of the concrete mixture, but However, the high economic cost of these fibers are an obstacle to the spread of use in our country is widely. The use of high-strength concrete at the present time are greater than normal concrete and that the effect of concrete resistance to pressure in a positive. The use of high-strength concrete (HSC) at the present time are greater than normal concrete (NSC) and that the effect of pressure on the resistance of the concrete low ratio of positive reinforcement, when the fiber-wrapped concrete is subjected to an axial compression loading, the concrete core expands laterally.

2. Background

The confinement pressure provided by the FRP increases continuously with the lateral strain of concrete because of the linear elastic stress-strain behavior of FRP. Failure of fiber-wrapped concrete generally occurs when the hoop rupture strength of the FRP is reached [1]. Several parameters, which include concrete strength, wrap thickness or number of FRP layers, and wrap angle orientation, influence the confinement effectiveness of FRP [2]. Many investigations have been conducted into the behavior of fiber-wrapped concrete and, as a result, a number of stress-strain models have been proposed. These models can be classified into two categories: (a) design-oriented models, and (b) analysis-oriented models, in the first category, the compressive strength, ultimate axial strain, and stress-strain behavior of fiber-wrapped concrete are predicted using closed-form equations based directly on the interpretation of experimental results. In the second category, stress-strain curves of fiber-wrapped concrete are generated using an incremental numerical procedure [3]. Li et al. [4] conducted an experimental study concrete cylinder confined; it was found that the strength, fibers oriented at a certain angle in between the transverse and longitudinal directions may result in strength lower than fibers along transverse or longitudinal directions. According to previous research on the subject there are a number of issues that need to be addressed : (a) how is the stress-strain behavior of concrete cylinders confined with CFRP composites, the answer is important in order to refine the existing design-oriented confinement models, (b) What are the effects of fiber orientation and wrap thickness on strength and ductility of concrete cylinders confined with CFRP composites, (c) How is the mode of failure, and Finally (d) how do dilation characteristics confined concrete perform with various fiber orientation. The present study is an experimental investigation of concrete cylinders confined with CFRP composites under axial loading. For answers to the above questions, a number of unreinforced concrete cylinders were prepared and confined with CFRP composites with different fiber orientations and various wrap thicknesses. Then an analytical modeling was performed on the stress-strain behavior of CFRP-confined circular concrete cylinders. Typical response of CFRP-confined concrete is shown in Fig. 1. Where normalized axial stress is plotted against axial, lateral, and volumetric strains, the stress is normalized with respect to the unconfined strength of concrete core the Figure shows that both axial and lateral responses are bi-linear with a transition zone at or near the peak strength of unconfined concrete core, the volumetric response shows a similar transition toward volume expansion .However, as soon as the jacket takes over, volumetric response undergoes another transition which reverses the dilation trend and results in volume compaction. This behaviour is shown to be markedly different from plain concrete.

3. Observed behavior of FRP-Confined cylinders

The confinement action exerted by the FRP on the concrete core is of the passive type, that is, it arises as a result of the lateral expansion of concrete under axial load. As the axial stress increases, the corresponding lateral strain increases and the confining device develops a tensile hoop stress balanced by a uniform radial pressure, which reacts against the concrete lateral expansion [5, 6]. When an FRP-confined cylinder is subject to axial compression, the concrete expands laterally and this expansion is restrained by the FRP. The confining action of the FRP composite for circular concrete cylinder is shown in Fig. 2. For circular cylinder, the concrete is subject to uniform confinement, and the maximum confining pressure provided by the FRP composite is

related to the amount and strength of FRP and the diameter of the confined concrete core, the maximum value of the confinement pressure that the FRP can exert is attained when the circumferential strain in the FRP reaches its ultimate strain and the fibers rupture leading to brittle failure of the cylinder, this confining pressure is given by:

$$f_l = (2 \epsilon_r E_f \epsilon_{fr} / d) \dots (1)$$

The CFRP volumetric ration is given by the following equation for fully wrapped circular cross section:

$$\rho_{FRP} = (4 \epsilon_r \epsilon_{fr} / d) \dots (2)$$

Failure model: Various confinement failure models have been proposed to predict the compressive failure strength of confined concrete cylinders, including the Richart model, N&N model, S&R model, MPP model, A&S model and Mirmiran model, most of them were proved by experiments. From of the equation: $f'_{cc} / f'_{co} = [1 + k (\epsilon_r / \epsilon_{fr})^m] \dots (3)$

Richart Model, [7]: suggested a linear relationship between the increases of failure strength of a confined concrete cylinder ($f_{cc} - f_{co}$) and the confining pressure f_r : $f'_{cc} = f'_{co} + k f_r \dots (4)$, N&N Model, [8]: suggested a nonlinear relationship between the failure strength and the confining pressure: $f'_{cc} = f'_{co} + \{3.7 * (f_r / f'_{co})^{0.14}\} \dots (5)$

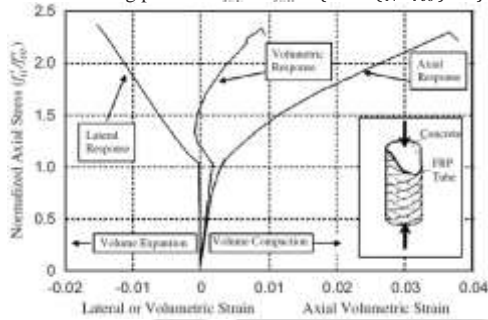


Fig. 1. Typical response of CFRP-confined concrete [24]

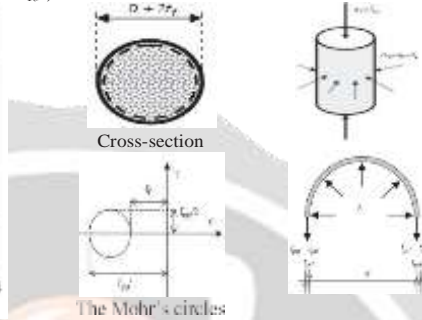


Fig. 2. Confinement action of FRP composite

S&R Model, [9]: suggested a different nonlinear relationship between the failure strength and the confining pressure based on the test data from Richart et al. (1928). $f'_{cc} = f'_{co} + \{6.7 * f_r\}^{0.17} * f_r \dots (6)$, MPP Model, [10]: also derived a nonlinear relationship between the failure strength and the confining pressure of confined concrete cylinder based on the triaxial test data. The MPP model is most widely used: $f'_{cc} = f'_{co} + [-1.254 + 2.54 * \sqrt{1 + (7.94 f_r / f'_{co})^2}] * f_r / f'_{co} \dots (7)$, A&S Model, [11]: suggested a linear relationship between the strength and the confining pressure of confined concrete cylinder based on the octahedral failure theory and test data. The proposed model is simplified to the following bilinear equations: $f'_{cc} = f'_{co} + \{1 + 4.2556 (f_r / f'_{co})\} \dots (8)$, Mirmiran Model, [12]: suggested the following relationship for FRP-encased concrete: $f'_{cc} = 4.2 * 69 (\epsilon_r / \epsilon_{fr})^{0.589} \dots (9)$

Fig. 3. The external and internal stress distribution of a confined concrete cylinder (a) concrete under axial loading, (b) concrete under confining pressure and (c) composite under confining pressure.

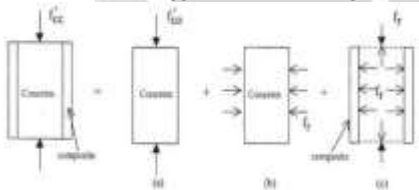


Fig. 3. The external and internal stress distribution of a confined concrete cylinder (a) concrete under axial loading, (b) concrete under confining pressure and (c) composite under confining pressure.

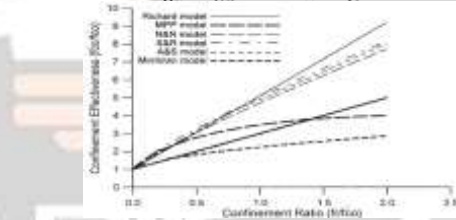


Fig. 4. Confinement effectiveness versus confinement ratio
Confinement types: Sufficient confinement with monotonic curve, with decreasing second part, Insufficient confinement

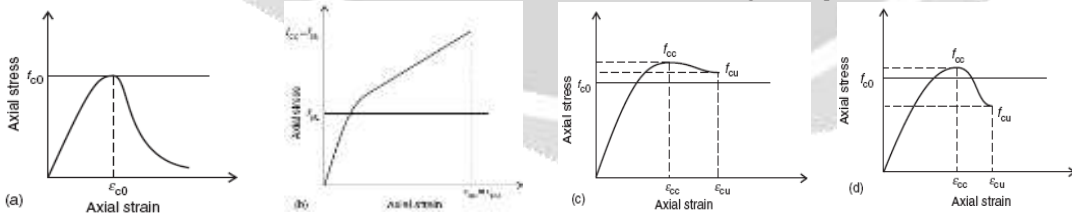


Fig. 5. (a) unconfined concrete; (b) sufficient confinement with monotonic curve; (c) sufficient confinement with decreasing second part; and (d) insufficient confinement,[3]

4. Experimental work:

Raw materials: (sand- crushed gravel) .Grain- size analysis test of aggregate: experiment was conducted (Grain- size analysis test of aggregate) 5 kg of gravel and 1 kg of sand: .Sand equivalent test: the experiment was conducted in sand equivalent of the sand used was SE = 87%. Specific surface of the cement: was the use of cement to produce a coefficient of Aleppo, a brand 52.5Mpa (brand

cement is the resistance of cement mortar on the pressure at the age of 28 days). Fig. 6, the experiment was conducted in cement mortar were verified resistance laboratory listed, as the experiment was conducted in the surface quality of the cement used was S = 3170 Cm2/gr. Abrasion of aggregate by use of the Los Angeles machine. Wear experiment was conducted in Los Angeles on the gravel material was used $C_{2.4} = 14\%$.

Table 1. Percentage passing sieve

sieve diameter [sand] mm	Percentage passing sieve
4.80	100
2.40	97
1.20	75
0.60	45
0.30	25
0.15	5



Fig. 6. sand equivalent experience and the surface quality of the cement and Los Angeles respectively

The mix composition of concrete consisted of 450 kg/m3 of cement, (Portland cement: CPA- CEM- I -R 52.5 Mpa). Qualitative and weighs 3150 kg/m3, W/C=29%. Air content 2.5 %, the maximum coarse aggregate diameter was 20 mm Table 2, show concrete mixture: Additional: Silica Fume 45kg/m3, Visconcrete tempo 12-High range water reducing and super plasticizing admixture: 1.55 L/m3 According to the specifications of U.S (ASTM C 494). Specimen preparations: The concrete was produced with a similar mixture design before casting in Standard cylindrical formworks.

Table 2. Concrete mixture proportions.

Mixture	Cement	Fine sand	Crushed gravel
Quantity kg/m3	350	390	1560
Ratio of cement %	100	111.43	445.7



Fig. 7. Silica fume and the Concrete Specimens

Slump of concrete = 4cm Measurements: Load cell Capacity 300 ton. LVDT number 2/. Compress meter-Extensometer (Standard: ASTM C469).



Fig. 8. Test cylinder unconfined concrete

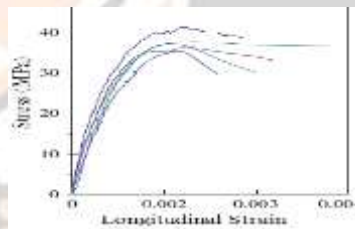


Fig. 9. Stress-Strain curves of specimens for unconfined cylinders

Results of the experiment on 15 cylinders, according to probability theory and mathematical statistics [13]:

$f'_{co} = f'_{cor} - k s ; f'_{cor} = \Sigma (f_i / n) ; s = \sqrt{\Sigma (f_i - \bar{f})^2 / (n - 1)}$ $n = 15 \Rightarrow k = 1.34 A = 17662.5 mm^2 s = 3.169$
 $f'_{co} (Mpa) = 46; 39; 40; 36; 38; 42; 39; 44; 44; 39; 44; 47; 42; 41; 39$ Fig. 9 shows the relationship between axial compression stress and strain longitudinal, scheme as well as axial compression stress and Lateral strain, of the unconfined cylinders. $f'_{co} (Mpa) = 41.4 ; f'_{co} (Mpa) = 37.15$. Values contained in the Table 3 are the average for stains /15/ cylinder, and the design of the relationship between stress and strain chart.

Table 3. (Longitudinal Lateral) strain for the unconfined cylinders

Cylinder Specimen	ϵ_{co} (Longitudinal) %	ϵ_{lt} (Longitudinal) %	ϵ_{co} (Lateral) %	ϵ_{lt} (Lateral) %
UC	2.65	2.93	0.54	0.61
rossion's ratio	0.205			
young's modulus	40529.05			

Table 4. Properties of unidirectional carbon fibres

Material type	Tensile Modulus (Gpa)	Density (g/cc)	Specific Modulus
HS Carbon	160-270	1.8	90-150
IM Carbon	270-325	1.8	150-180
HM Carbon	325-440	1.8	180-240
UHM Carbon	> 440	2.0	> 200

4.1. CFRP Materials:

Types of carbon fibers. Fig.10 :



Fig. 10. types of CFRP

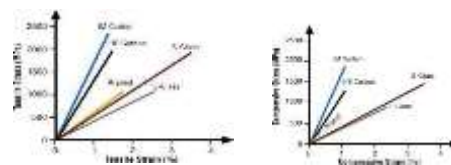


Fig. 11. a: tensile strength, b: compression strength

By type young modulus: show table .4, Reduced strength and endurance on the pressure in the fiber on the tensile strength by 80%, Fig. 11 : The carbon fiber sheets used in this study were the SikaWrap- 230C product, a unidirectional wrap, the manufacturer's guaranteed tensile strength for this carbon fiber is (2500-3000) Mpa, with a ultimate tensile modulus of >210 GPa, ultimate elongation of 1.6%, and a sheet thickness of 0.165mm, the resin system that was used to bond the carbon fabrics over the cylinders in this work was the epoxy resin made of two-parts, resin and hardener, the mixing ratio of the two components by weight was 4: 1, the properties of the resin are given in Table 5 (data are given by the manufacturer), SikaWrap-230C was field laminated using Sikadur-330 epoxy to form a CFRP wrap used to strengthen the concrete specimens.

Table 5. The manufacturer's Mechanical properties of CFRP and resin

	CFRP	Resin
Ultimate Tensile strength (Mpa)	2500-3000	>30 at 2 days and 20 C
Elastic Modulus (Gpa)	>210	4.5 at 7 days and 23 C
Ultimate elongation in tensile %	1.6	0.9
Compressive stress (Mpa)	-	>55 at 2 days and 20 C
Areal weight (g/m2)	332	-

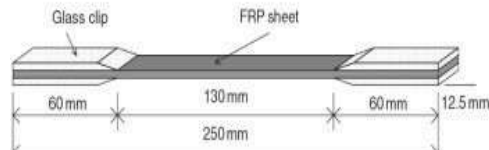


Fig. 12. Dimensions of flat coupons for tensile testing

4.2. Test CFRP properties:

to verify the mechanical properties of carbon fibers, tensile experiment was conducted on a sample of standard carbon fiber, (ASTM D3039) the test coupon specimens had a length of 250mm including two 60 mm glass clips and a width of 12.5 mm Fig.12 shows the dimensions of the test specimens in detail, The experience of tensile fiber, samples of fiber-way single: Used in this research are three types of carbon fiber, the first type (fiber in one direction) is horizontal ($\theta = 0^\circ$), and vertical ($\theta = 90^\circ$), the second type (carbon fiber two-way ($\theta = 0^\circ/90^\circ$), the third type (Four directions), ($\theta = 0^\circ/90^\circ & \pm 45^\circ$).Fig. 14.

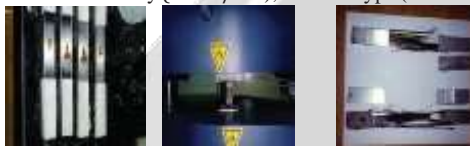


Fig. 13. Test CFRP (tensile strength)



Fig. 14 .CFRP (one-way, two-way, four-way) respectively

Tensile strength of CFRP laminate strips were within the range of the manufacturer's published values, in order to verify the properties of resin used, casting cubes / $5 \times 5 \times 5$ /cm according to the rules of (ASTM-C109-88) Samples in the tensile character 8 according to the rules (ASTM-C190-85).

Table 6. Average results of CFRP fabric
t_f 0.165 mm

Fibre orientation	Ultimate strength (Mpa)	Initial modulus (Gpa)	Ultimate Strain %
Longitudinal orientation $\theta = 0^\circ$	2100	230	1.6

Table 7. Properties of the Resin and Hardener

Properties	Ultimate strength (M)
Tension	76.1
Compression	97.4

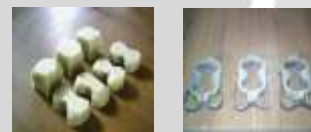


Fig. 15. Resin samples

4.2. CFRP Wrapping :

(CFRP confined cylinder preparation) configurations of CFRP wrapping, the surface of the specimen was ground to remove loosely held powders, and was then cleaned with water and left to dry, before wrapping, the concrete surface was coated with a layer of epoxy primer; a layer of epoxy resin was next applied on the surface of the specimen 2-3 h after coating the primer when the primer was not yet completely dry, this was followed by wrapping continuous carbon/epoxy laminates around the specimen with the fibers oriented in the hoop direction, forming one to three layers (n=3) of CFRP with each layer containing a single lap of fiber sheet, as the width of a single sheet available to the authors was not sufficient to cover the entire length of a specimen, two separate sheets were used for the upper and lower parts of each specimen respectively, without overlapping at the circumferential seam, after the wrapping of each lap of fiber sheet, a layer of epoxy resin was applied and a screw roller was used to remove air voids and to allow a better impregnation of the resin. The finishing end of each sheet overlapped the starting end of the sheet by 100 mm, Fig.16. According to the rules ASTM D7616 / D7616M -11.

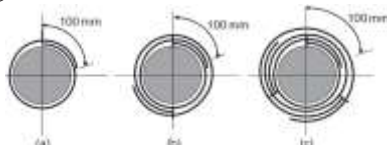


Fig. 16. CFRP Wrapping: (a) single type : (b) two type: (c) three type

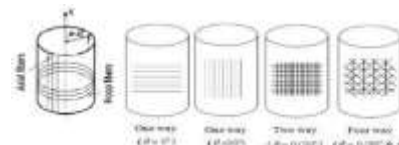


Fig. 17. Fiber Orientation in CFRP-Wrapped Cylinders.

The wrapped specimens were exposed to the laboratory environment at room temperature for the CFRP to cure for at least seven

days before testing, as suggested by the material manufacturer ,CFRP Orientation Angle:

Table 8. Test program and specimen properties

Specimen (abbreviation)	Number of layers	Fibre orientation	Total Number
One way (horizontal)(OWH)	One Two Three	$\theta = 0^\circ$	9
One way (vertical) (OWV)		$\theta = 90^\circ$	9
Two way (TW)		$\theta = 0^\circ/90^\circ$	9
Four way (FW)		$\theta = 0^\circ/90^\circ \& \mp 45^\circ$	9



Fig. 18. Typical failure modes of CFRP-confined concrete cylinders

4.3. Failure Mode:

All the CFRP-wrapped cylinders failed by the rupture of the FRP jacket due to hoop tension. The CFRP-confined specimens failed in a sudden and explosive manner and were only preceded by some snapping sounds. Many hoop sections formed as the CFRP ruptured.

These hoops were either concentrated in the central zone of the specimen or distributed over the entire height, as can be seen in Fig.18. The wider the hoop, the greater the section of concrete that remained attached to the inside faces of the delaminated CFRP. None of the specimens failed at the overlap location of the jacket, which confirmed the adequate stress transfer over the splice.

The following Table 9 shows comparison of factor confined for researchers (MPP Model, Richart Model, N&N Model, S&R Model, A&S Model, Mirmiran Model). With the percentages of error for the experimental work.

Table 9 .Comparison of predicted strength with experimental data
 $t_f = 0.165 \frac{f_{FRP}}{f_{c,c}} \cdot f_{c,c} = MPP$

Unit (Mpa)	One Layer of Carbon	Two Layers of Carbon	Three Layers of Carbon
Experiment	49.0	68.0	83.2
MPP Model (error)	64.0 (30%)	82.8 (21%)	95.2 (14%)
Richart Model (error)	60.8 (24%)	91.8 (35%)	122.9 (27%)
N&N Model (error)	63.5 (29%)	91.1 (34%)	116.9 (40%)
S&R Model (error)	65.5 (33%)	93.4 (37%)	118.9 (43%)
A&S Model (error)	61.8 (26%)	94.1 (38%)	123.5 (48%)
Mirmiran Model (error)	43.7 (-11%)	50.8 (-25%)	56.4 (-32%)

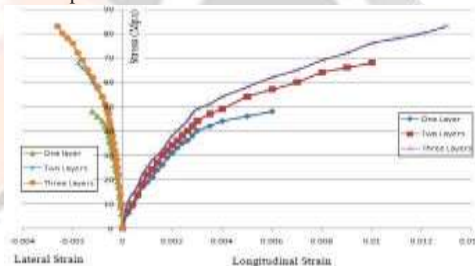


Fig. 19. Diagram stress - strain (Longitudinal - Lateral) of the confinement cylinders at an angle zero (OWH).

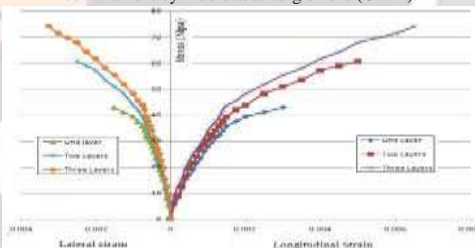


Fig. 20. Diagram stress - strain (Longitudinal - Lateral) of the confinement cylinders at an angle 90, (OWV)

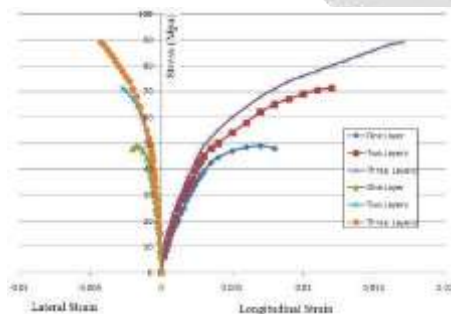


Fig. 21. Diagram stress - strain (Longitudinal - Lateral) of the confinement cylinders at Dual fibre, (TW)

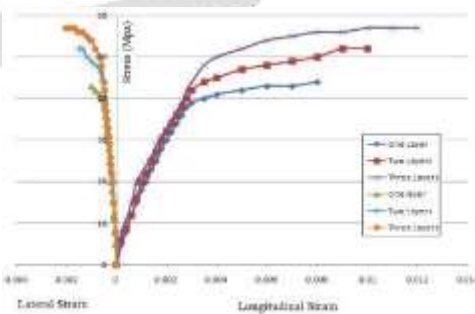


Fig. 22. Diagram stress - strain (Longitudinal - Lateral) of the confinement cylinders at fiber quartet, (FW)

5. Analytical study

Finite element analysis: The ANSYS FE [15] Software was used for 3D modeling of CFRP-wrapped concrete cylinders; all cylinders were 150 mm by 300 mm and were subjected to axial compression. Element type: Reinforced concrete (Solid65.Fig.23).The criterion for failure of concrete due to a multiaxial stress state can be expressed in the form (William and Warnke1975) [16]. Solid65 element has been used to model concrete in the present study; the element has eight nodes with three degrees of freedom at each node.

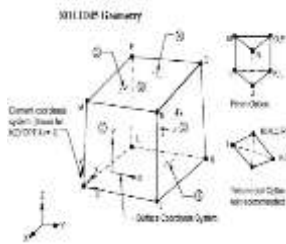


Fig. 23. Solid65 element [15]

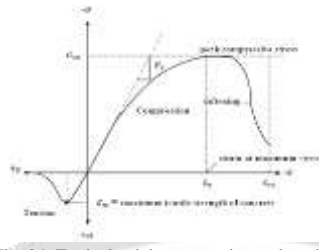


Fig. 24. Typical axial compressive and tensile stress-strain curve for concrete (Bangash 1989)[18]

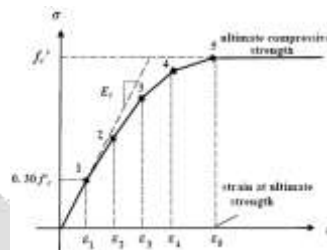


Fig. 25. stress-strain curve for the concrete [15]

The element of plastic deformation, cracking in three orthogonal directions, and crushing, the linear behavior of concrete, as obtained by using Solid65, development of a model for the behavior of concrete is a challenging task, concrete is a quasi brittle material and has different behavior in compression and tension, the tensile strength of concrete is typically 8 -15% of the compressive strength (Shah, et al. 1995), [17]. Fig. 24. Shows a typical stress-strain curve for normal weight concrete (Bangash 1989[18]), in compression, the stress-strain curve for concrete is linearly elastic up to about 30 percent of the maximum compressive strength, above this point, the stress increases gradually up to the maximum compressive strength, after it reaches the maximum compressive strength f_{cu} , the curve descends into a softening region, and eventually crushing failure occurs at an ultimate strain ϵ_u in tension, the stress-strain curve for concrete is approximately linearly elastic up to the maximum tensile strength, after this point, the concrete cracks and the strength decreases gradually to zero (Bangash 1989) [18].The following properties must be entered in ANSYS: elastic modulus $E_c = \sqrt{f_{cu}}$ [13], ultimate axial compressive f'_{cu} , Poisson's ratio $\nu = 0.2$, ultimate Uniaxial tensile strength $= 0.44\sqrt{f_{cu}}$ [13] Shear transfer coefficient β , which is represents conditions of the crack face, the value of β ranges from 0.0 to 1.0, with 0.0 representing a smooth crack (complete loss of shear transfer) and 1.0 representing a rough crack (no loss of shear transfer) [15]. The shear transfer coefficient used in present study varied between 0.3 and 0.4. The present study assumed that the concrete is a homogeneous and initially isotropic, compressive axial stress-strain relationship for concrete model is obtained by using the following equations to compute the multilinear isotropic stress-strain curve for the concrete is as shown in Fig. 25, The curve starts at zero stress and strain. Point 1, at $0.3f_c$, is calculated for the stress-strain relationship of the concrete in the linear range (must satisfy Hooke's law), $f'_c = \epsilon * E_c$ for $0 \leq \epsilon \leq \epsilon_1 \dots (10)$, Points 2, 3, and 4 are obtained from equation: $f'_c = \epsilon * E_c / 1 + (\epsilon/\epsilon_1)^2$ for $0 \leq \epsilon \leq \epsilon_1 \dots (11)$, Point 5 is at ϵ_5, f'_c , the behaviour is assumed to be perfectly plastic after point 5: $\epsilon = 2 / f'_c \dots E_c (12)$. Finite element idealization CFRP composites (solid46): An assumption commonly made in FRP modeling is that FRP is a linear elastic material until it reaches its tensile strength and has orthotropic material properties, even when a very large pressure load such as a blast load is applied, it is commonly assumed that FRP is a order to consider the directional characteristics of FRP, it has to be modeled as an orthotropic material, if this is the case, then a linear elastic orthotropic material model has at least two symmetrical orthogonal planes as shown in Fig 26. Input data needed for the FRP composites in the finite element models are as follows: number of layers, thickness of each layer, orientation of the fibber direction for each layer, elastic modulus of the FRP composite in three directions (Ex, Ey and Ez), Shear modulus of the FRP composite for three planes (Gxy, Gyz and Gxz), Major Poisson's ratio for three planes (vxy, vyz and vxz).

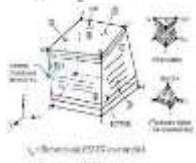


Fig. 26. composites (solid46) element [15]

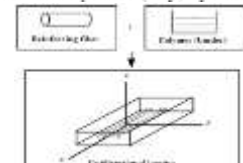


Fig. 27. Schematic of FRP composites (Gibson 1994, Kaw 1997)[22,23]

Table 10. Summary of material properties for CFRP composites

Materials	Elastic modulus Gpa	Major Poisson's ratio	Shear modulus Mpa
CFRP	$E_x = 200$	$\nu_{xy} = 0.22$	$G_{xy} = 3270$
One way	$E_y = 48$	$\nu_{xz} = 0.22$	$G_{xz} = 3270$
	$E_z = 48$	$\nu_{yz} = 0.3$	$G_{yz} = 1860$

CFRP composites are materials that consist of two constituents. The constituents are combined at a macroscopic level and are not soluble in each other. One constituent is the reinforcement, which is embedded in the second constituent, a continuous polymer

called the matrix (Kaw1997) [22], the reinforcing material is in the form of fibres, i.e., carbon and glass, which are typically stiffer and stronger than the matrix. The FRP composites are anisotropic materials; that is, their properties are not the same in all directions. Fig 27 shows a schematic of FRP composites. Note that a local coordinate system for the FRP layered solid elements is defined where the x direction is the same as the fiber direction, while the y and z directions are perpendicular to the x direction. The properties of isotropic materials, such as elastic modulus and Poisson's ratio, are identical in all directions, therefore no subscripts are required, this is not the case with specially orthotropic materials, subscripts are needed to define properties in the various directions, for example E_x , E_y and ν_{xy} is the elastic modulus in the fibre direction, and E_y is the elastic modulus in the y direction perpendicular to the fibre direction, the use of Poisson's ratios for the orthotropic materials causes confusion, therefore the orthotropic material data are supplied in the ν_{xy} or major Poisson's ratio format for the ANSYS program, the major Poisson's ratio is the ratio of strain in the y direction to strain in the perpendicular x direction when the applied stress is in the x direction, the quantity ν_{xy} is called a minor Poisson's ratio and is smaller than ν_{yx} whereas E_x is larger than E_y . Equation (16) shows the relationship between ν_{xy} and ν_{yx} (Kaw 1997) [22] $\nu_{yx} = (E_y / E_x) \nu_{xy}$... (16), where ν_{yx} Minor Poisson's ratio, E_x Elastic modulus in the x direction (fiber direction). E_y = Elastic modulus in the y direction. ν_{xy} Major Poisson's ratio, Action Steps program Ansys: Preprocessor>element type-material props- section-modeling-meshing. Solution > analysis type-define loads- solve-analysis nonlinear. General Postproc>real constants- results viewer Fig. 28 shows the modeling process and the division and load forces and restrictions.

Table 11. Strains in cylinders studied (program ANSYS)

Cylinder Specimen	NO. CFRP layers	f_{cc} Mpa	ϵ_{cc} %	ϵ_u %	f_{cu} Mpa	ϵ_{cc} %	ϵ_{cu} %	f_{cc} / f_{cu}	$\epsilon_{cc} / \epsilon_{cu}$	$\epsilon_{cu} / \epsilon_u$
UC	-	37.2	2.65	3.00	-	-	-	-	-	-
CC (OWH)	1	=	=	=	48.6	8.2	10.7	1.31	3.09	3.57
	2	=	=	=	64.7	10.5	10.5	1.74	3.96	3.5
	3	=	=	=	71.4	13.5	13.5	1.92	5.09	4.5
CC (OWV)	1	=	=	=	43.1	3.34	3.34	1.16	1.26	1.11
	2	=	=	=	54.4	5.98	5.98	1.46	2.26	1.99
	3	=	=	=	63.2	7.21	7.21	1.70	2.72	2.40
CC (TW)	1	=	=	=	49.3	6.41	6.41	1.33	2.42	2.14
	2	=	=	=	65.8	10.2	10.2	1.77	3.85	3.4
	3	=	=	=	76.9	12.5	12.5	2.07	4.72	4.17
CC (FW)	1	=	=	=	42.9	8.2	8.2	1.15	3.09	2.73
	2	=	=	=	50.3	10.7	10.7	1.35	4.03	3.57
	3	=	=	=	56.1	13.1	13.1	1.51	4.94	4.37

$n_t=0.165$ for one layer, $n_t=0.33$ for two layer, $n_t=0.495$ for three layer

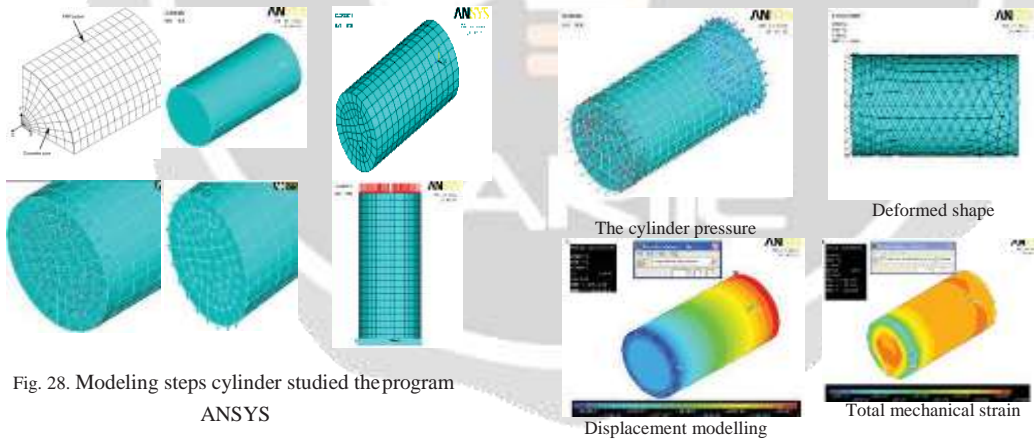


Fig. 28. Modeling steps cylinder studied the program ANSYS

Fig. 29. Displacements and Strains in cylinder studied the program ANSYS

6. Discuss the results

- 1- The amount of the maximum rate of increase in the energy f_{cc} / f_{cu} of the studied cylinder pressure as a result of an act confined to carbon fiber / 2.23 / experimental, Fig (21-22). The analytical value of /2.07/, Table 11, and for the three layers of fibre bilateral.
- 2-Ranged from the difference between the analytical and experimental study of the limits / 7-12 /%.
- 3- Increase the ratio of effective power fiber-wrapped cylinders f_{cc} / f_{cu} to increase resistance to Pressure and increase fibre thickness, A comparison was made between the percentage f_{cc} / f_{cu} (Confinement Effectiveness) and thickness of the fibre

with resin, for a number of resistors f'_{cc} . Fig.30

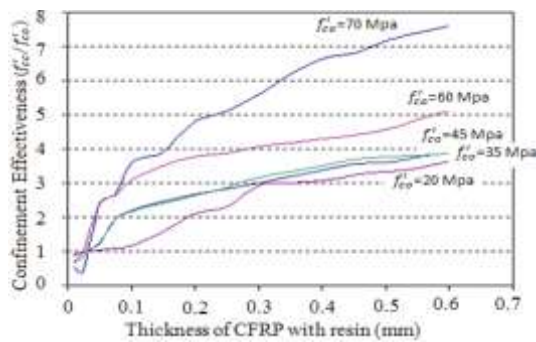


Fig. 29. Chart shows the relationship between confinement effectiveness and thickness of CFRP for a number of resistors

- 4- Resistance to different fiber-wrapped cylinder pressure according to the orientation angle of fiber, and using the horizontal fiber, was reduced lateral strain Fig.19, and thus contributed to the increased resistance of the concrete cylinders compared with the same fiber, but in a vertical.
- 5- Increased ultimate strain in cylinders wrapped by fiber /4.5/, and for the fiber-wrapped cylinders are horizontal and three layers, and that the value of / 0.003 / to value / 0.0135 /, this explains the tensile strength fibers that surround the concrete.
- 6- Fiber quartet gave lower yields for the strengthening of the pressure compared to horizontal and vertical fiber.
- 7- The study being updated, as are a set of additional tests to determine the effect of other factors such as tweaking the partial cylinder plates of CFRP, and economic feasibility, and the results will be presented in a subsequent study.

7. Conclusions

The purpose of the experimental work involved in this study was mainly to evaluate the effectiveness of strengthening plain- and RC cylinders with CFRP composite. Based on the analysis of experimental results, the following conclusions are made:

- 1- The finite element analysis performed in this study demonstrated that externally bonded CFRP reinforcement is a viable solution towards enhancing the strength and ductility of concrete cylinders subjected to axial load. Parameters considered include the wrap thickness and the wrap configuration, which includes combination of 0 and ± 45 ply angles with respect to the circumferential direction and the ply stacking sequence.
- 2- In the present study effectiveness of CFRP laminates in improving the compressive strength of concrete cylinders was presented. It was observed that CFRP laminates, if used for confinement of concrete cylinders, can improve the axial and lateral strength of concrete cylinders dramatically. However, the percentage increase depends on number of layers of CFRP laminates, used for wrapping the cylinder, and compressive strength of concrete. It was further observed that the percentage increase in compressive strength was more for normal strength concrete than that in high-strength concrete.
- 3- Effect of confinement on ductility was also studied and it was observed that: (a) CFRP laminate wrapping increases not only the strength but also the ductility considerably; (b) for given mix, ductility is more for three layered confinement than single layered confinement; and (c) for given confinement, ductility is higher for normal strength concrete than high strength concrete.
- 4- Fiber orientation and FRP wall thickness have a considerable effect on the stress-strain behavior, strength, ductility, and failure mode of wrapped concrete cylinders. The CFRP confinement effect cannot be fully realized without proper fiber orientation and sufficient wall thickness.
- 5- Insufficient confinement results in almost no increase in strength. Insufficient confinement must be avoided in practice. Otherwise, it is a waste of materials and may lead to premature structural failure.
- 6- The average hoop strain in FRP at rupture in FRP-wrapped concrete can be much lower than the FRP material ultimate tensile strain supplied by manufacturers, indicating the assumption that FRP ruptures when the FRP material tensile strength reached is not valid in the case of concrete confined by FRP wraps. Based on this observation, an effective peak stress and corresponding strain formula for concrete confined by FRP must be based on the actual hoop rupture strain of FRP rather than the ultimate material tensile strain.
- 7- Failure of all confined cylinders is marked by the rupture of carbon fibers. It occurs prematurely, for stress level appreciably lower than the ultimate strength of the CFRP composite.

References

- [1] Teng, J. G. and Lam, L. (2004). Behavior and Modeling of Fiber Reinforced Polymer-Confined Concrete. *Struct. Eng. ASCE*, 130(11): 713-723.
- [2]- Parvin, A. and Jamwal, A. S. (2005). Effects of Wrap Thickness and Ply Configuration on Composite-Confined Concrete Cylinders *Compos Struct.*, 67(4): 437-442.
- [3]- Lam, L. and Teng, J. G. (2003). Design-Oriented Stress Strain Model for FRP-Confined Concrete, *Constr.Build. Mater.*, 17(6&7): 471-489.
- [4]- Li, G., Maricherla, D., Singh, K., Pang, S. and John, M. (2006). Effect of Fiber Orientation on the Structural Behavior of FRP Wrapped Concrete Cylinders, *Composite Structures*, 74(4): 475-483.
- [5]-De Lorenzis, L. and Tefers, R. (2001). A Comparative Study of Models on Confinement of Concrete Cylinders with FRP Composites, Division of Building Technology, Work No.46, p. 81, Publication:01:04, Chalmers University of Technology, Sweden
- [6]-Teng, J. G., Chen, J. F., Smith, S. T. and Lam, L. (2002). *FRP Strengthened RC Structures*, p. 245, John Wiley and Sons Ltd., Chichester, UK
- [7]-Richart, F. E., A. Brandtzaeg and R. L. Brown. 1928. "A Study of the Failure of Concrete under Combined Compressive Stresses," *Engrg. Experimental Station Bull. No. 185*, University of Illinois, Urbana, Illinois
- [8]-Newman, K. and J. B. Newman. 1971. "Failure Theories and Design Criteria for Plain Concrete," *Proc., Int. Civil Engrg. Mat. Conference on Structure, Solid Mech. and Engrg. Des.* Wiley Interscience, New York, NY, pp. 936-995.
- [9]-Saaticioglu, M. and S. R. Razvi. 1992. "Strength and Ductility of Confined Concrete," *Journal of Structural Engineering, ASCE*, 118:1590-1607.
- [10]-Mander, J. B., M. J. N. Priestley and R. Park. 1988. "Theoretical Stress-Strain Model for Confined Concrete," *Journal of Structural Engineering, ASCE*, 114:1804-1823
- [11]-Ahmad, S. H. and S. P. Shah, 1982. "Complete Triaxial Stress-Strain Curves for Concrete. *Journal of Structural Division*," Proceedings of the American Society of Civil Engineering, ASCE, 108(ST4):728-742.
- [12]-Mirmiran, A. 1996. "Analytical and Experimental Investigation of Reinforced Concrete Columns Encased in Fiberglass Tubular Jackets and Use of Fiber Jacket for Pile Splicing," Final Report, Contract number B9135, Florida Dept. of Tallahassee, Fla
- [13]- Syrian Arab Code (2004), Engineers Syndicate, Design and Construction, Third edition, page 32-33.
- [14]-ACI Committee 440 Report (2002). Guide for the Design and Construction of Externally Bonded FRP Systems for Strengthening Concrete Structures. ACI Committee 440, Technical Committee Document 440.2R-02.
- [15] - ANSYS User's Manual 11.0, Release 11.0, ANSYS, Inc., 2007
- [16]-William, K.J. and Warnke, E. D., "Constitutive Model for the Triaxial Behavior of Concrete", Proceedings, International Association for Bridge and Structural Engineering, Vol. 19, ISMES, Bergamo, Italy, p. 174 (1975).
- [17]- Shah, S. P., Swartz, S. E., and Ouyang, C., *Fracture Mechanics of Concrete*, John Wiley & Sons, Inc., New York, New York, 1995
- [18]- Bangash, M. Y. H., *Concrete and Concrete Structures: Numerical Modeling and Applications*, Elsevier Science Publishers Ltd., London, England, 1989.
- [19]- ACI 318m-05, American Concrete Institute, (2005) Building Code Requirements for Reinforced Concrete, American Concrete Institute, Farmington Hills, Michigan.
- [20]-Mindess, S. and Young, J. F., *Concrete*, Prentice-Hall, Inc., Englewood Cliffs, New Jersey, 1981.
- [21]-Shah, S. P., Swartz, S. E., and Ouyang, C., *Fracture Mechanics of Concrete*, John Wiley & Sons, Inc., New York, 1995.
- [22]- Kaw, A. K., *Mechanics of Composite Materials*, CRC Press LLC, Boca Raton, Florida, 1997.
- [23]- Gibson, R. F., *Principles of Composite Material Mechanics*, McGraw-Hill, Inc, New York, 1994.
- [24]- Mirmiran A, Zagers K, Yuan W. Nonlinear finite element modeling of concrete confined by fiber composites. *Finite Elements in Analysis and Design* 2000;35:79-96.
- [25]- ANSYS User's Manual 9.0, Release 9.0, ANSYS, Inc., 1998.